A&A 520, A41 (2010)
DOI: 10.1051/0004-6361/201014329

Astronomy & Astrophysics

Implications of a new triple-α nuclear reaction rate

Consequences for Cepheids

P. Morel[1], J. Provost[1], B. Pichon[1], Y. Lebreton[2,3], and F. Thévenin[1]

[1] Université de Nice-Sophia Antipolis, CNRS UMR 6202, Observatoire de la Côte d'Azur, Laboratoire Cassiopée, BP 4229, 06304 Nice Cedex 04, France
e-mail: [Pierre.Morel;Janine.Provost;Bernard.Pichon;Frederic.Thevenin]@oca.eu
[2] Observatoire de Paris, Laboratoire GEPI, CNRS UMR 8111, 92195 Meudon, France
e-mail: Yveline.Lebreton@obspm.fr
[3] IPR, Université de Rennes 1, 35042 Rennes, France
e-mail: Yveline.Lebreton@univ-rennes1.fr

Received 26 February 2010 / Accepted 13 June 2010

ABSTRACT

Context. Recently the triple-α reaction rate has been re-evaluated. In the temperature range, 10^7-10^8 K, with respect to the NACRE rate, the new rate is enhanced by up to 20 orders-magnitude.
Aims. To validate this new rate, we investigate its consequences for the evolution of Cepheid models.
Methods. The stellar evolutionary tracks are calculated with the CESAM code and displayed in the domain 4–10 $M_\odot$.
Results. With the new rate, the first dredge-up does not occur. For masses larger than $\gtrsim$4.5 $M_\odot$ each evolutionary track crosses the instability strip only once. The luminosities are higher than with the previous rate, then leading to smaller theoretical masses that better agree with the pulsational mass. Conversely, and inconsistently with one century of observations of more than two hundred Cepheids, the temporal derivative of the period keeps a positive sign. Moreover the observed depletions of atmospheric lithium and C/N ratio do not occur. A slight modification of only a few percents of the new nuclear rate allows us however to restore the loops inside the instability strip and the changes of sign of the temporal derivative of periods.
Conclusions. This preliminary work indicates that the new rate may solve some of the long-lasting unsolved theoretical problems of Cepheids. Yet indisputable observations argue against its pertinence. Nonetheless, with regard to its theoretical importance, the triple-α new reaction rate still needs to be confirmed or revisited.

Key words. nuclear reactions – nucleosynthesis – abundances – stars: evolution – stars: variables: Cepheids

1. Introduction

Recently, Ogata et al. (2009, hereafter OKK) have re-evaluated the triple-α (3α) reaction rate by directly solving the three-body Schrödinger equation. In the temperature range 10^7 K – 2×10^8 K they obtained a rate enhanced by up to 20 times compared to the rate provided in the NACRE (Angulo et al. 1999) compilation. Ogata et al. (2009) give the new rate $3\alpha_{\rm OKK}$ as a tabulated correction $\Delta3\alpha$ to be applied to the rate of NACRE $3\alpha_{\rm NACRE}$:

$$\log_{10}(3\alpha_{\rm OKK}) = \log_{10}(3\alpha_{\rm NACRE}) + \log_{10}(\Delta3\alpha). \quad (1)$$

Figure 1 shows the 3α reaction rates computed with the NACRE and OKK requirements respectively. It is accepted up to now that the ignition of the 3α reactions occurs at temperatures $T \gtrsim 100$ MK (Kippenhahn & Weigert 1991). At these temperatures its rate amounts to 2.38×10^{-24} cm^3 mol^{-1} s^{-1} according to NACRE. With the OKK new rate, this level corresponds to a temperature close to $T \sim 50$ MK. Hereafter we will designate by *cold helium burning* (CHeB) the OKK rate in contrast to the *hot helium burning* (HHeB) of the NACRE reaction rate. The 3α helium burning occurs in physical conditions unattainable for experimental validation except in stellar interiors. As seen in Fig. 2 left panel, the HR diagram would need to be revisited if this new 3α rate was really at work in stars.

Saruwatari & Hashimoto (2008) have investigated the theoretical effects of the OKK new 3α rate on helium ignition for white dwarfs in accretion binary systems, considered as progenitors of type Ia supernovae.

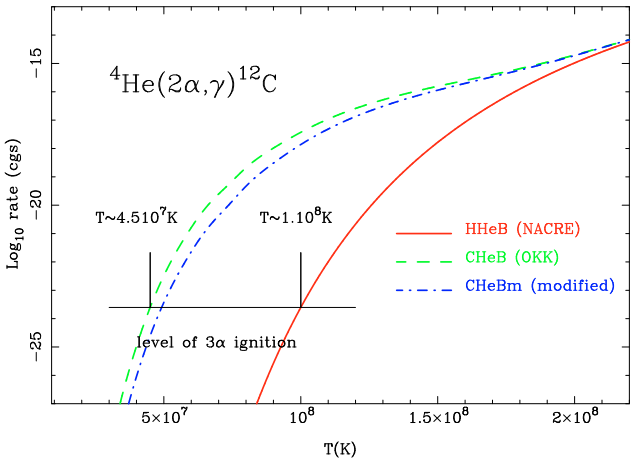

Fig. 1. (Colour online) The NACRE (full) and enhanced Ogata et al. (2009) (dash) triple-alpha reaction rates variations with temperature. With OKK, the temperature of the ignition is about halved. For CHeBm (dot-dash) the correction $\log_{10}(\Delta3\alpha)$ is arbitrarily reduced by 7% – see Sect. 5.

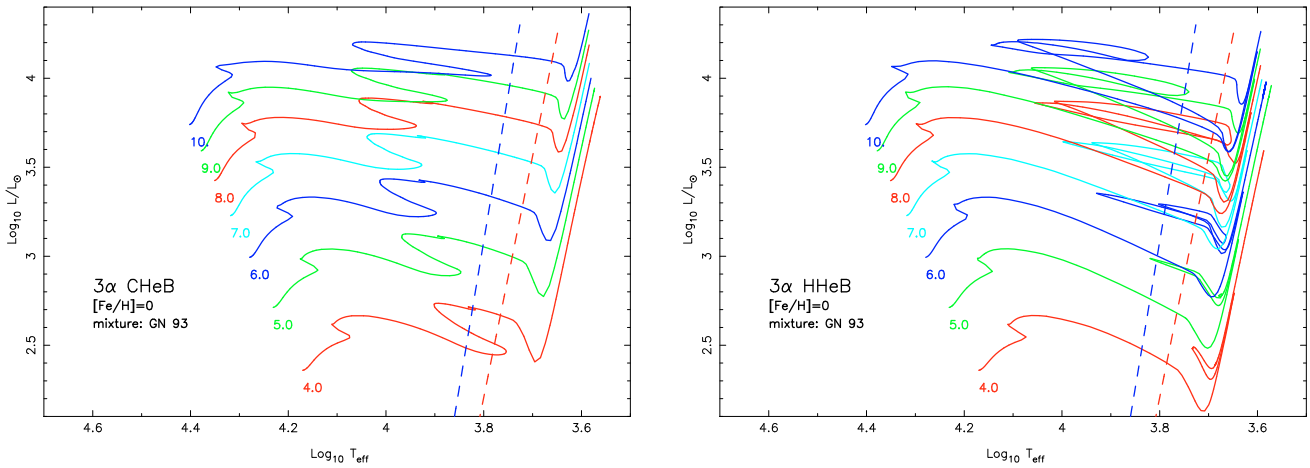

Fig. 2. (Colour online) *Left panel*: evolutionary tracks computed with cold helium burning (CHeB). *Right panel*: evolutionary tracks computed with hot helium burning (HHeB). The left and right dashed lines respectively delimit the blue and red sides of the Cepheids instability strip. For clarity only the part of the evolutionary tracks beyond the ZAMS is displayed.

Dotter & Paxton (2009) found that the OKK rate is incompatible with the evolution of late-type stars through the helium flash and the existence of extended red giant branches in old stellar systems. In these stars the 3α ignition occurs in a degenerate medium. Yet even with a temperature sensitivity $\propto T^{26}$ for CHeB, instead $\propto T^{40}$ for HHeB, the 3α ignition remains explosive and the numerics are unstable.

Precisely because their pulsations occur during the helium burning in their core, the Cepheids are promising objects for exhibiting quantitative tests for the new rate. Cepheids are important because the period of their pulsation is related to their luminosity, they have been long recognized as primary standards to estimate the distances. They still are subjects of numerous theoretical and observational galactic and extra galactic works based on observations stretched over more than a century. The Cepheids pulsate when they are located in a wedge-shaped area of the Hertzsprung-Russell diagram, the so-called *"instability strip"* (Turner 2001). Its width is of the order of $\Delta \log_{10} T_{\rm eff} \sim 0.09$. Despite the huge theoretical investment two points remain unexplained:

1. these stars pulsate when they describe one or several *"blue loops"* through the instability strip. But the physical conditions for the existence and extent of blue-loops are still debated (Kippenhahn & Weigert 1991; Valle et al. 2009). As an example, in our calculations with the opacities and the solar mixture of Asplund et al. (2005), blue loops cross the instability strip only for masses larger than $\sim 7\ M_{\odot}$;
2. since the late sixties it became apparent that the masses of Cepheids predicted from the theory of stellar evolution were larger than those predicted by the pulsation theory (Cox 1980). Nowadays this problem remains open (Caputo et al. 2005; Valle et al. 2009, and references therein). The most currently invoked physical process to explain these discrepancy is the existence during the main sequence hydrogen burning phase of a hypothetical core overshoot in the range of 0.2 to 0.8 pressure scale height (Keller 2008, and references therein). The overshooting produces a larger helium core, it increases the amount of helium nuclear fuel available during the pulsation. The higher the convective core overshoot, the larger the luminosity for a given mass or conversely for a given luminosity the smaller the theoretical mass. Mass loss occurring just before the Cepheid's pulsation phase is also invoked to reduce the theoretical mass (Valle et al. 2009, and references therein). None of these physical processes are clearly understood or quantified up to now.

Hereafter we study how models of Cepheids computed with CHeB are modified and if these models may provide answers to these open questions.

The paper is organized as follows. In Sect. 2 we present the physical processes, physical data, values of parameters and numerical techniques used. Section 3 is devoted to a description of evolutions using CHeB and HHeB with emphasis on models with the mass of δ Cephei (i.e. $\simeq 6.6\ M_{\odot}$). A discussion of results is made in Sect. 4. Results of numerical experiences with changes of physical data are briefly reported in Sect. 5. Conclusions are given in Sect. 6.

2. Methods

Our goal is to investigate in a general way the consequences of the 3α new rate on Cepheid models. Fixing the physics and the numerics, we have calculated several stellar models with characteristic masses of Cepheids.

Calculation of models: The models were computed with the CESAM2k code (Morel 1997; Morel & Lebreton 2008). The evolutions were initialized with homogeneous pre-main sequence models. The EFF equation of state (Eggleton et al. 1973) was used, together with opacities determined by Iglesias & Rogers (1996) using the solar mixture of Grevesse & Noels (1993), complemented at low temperatures by Alexander & Ferguson (1994) opacities. Conductive opacities were taken from Iben (1975). We used the composition $X = 0.7126$, $Y = 0.270$, ($Z = 0.0174$, $Z/X = 0.0244$). In the convection zones the temperature gradient was computed according to the Canuto & Mazitelli (1991) convection theory with the mixing length parameter set to unity as recommended by these authors. The atmosphere was restored using Eddington's atmospheric law (Mihalas 1978). The relevant nuclear reaction rates of pp chain, CNO and 3α cycles were taken from the NACRE compilation. Mass loss, rotation, microscopic and turbulent diffusion are not included in the models. Overshooting is only considered in Sect. 5. For models computed with CHeB, the analytical

form of the 3α reaction rate from NACRE is enhanced in accordance with Ogata et al. (2009) data and interpolated according to Eq. (1).

Period: in a first approximation the period p (in days) of Cepheids depends on the mean density (Cox 1980):

$$p = \bar{Q}_i \sqrt{\frac{R^3}{M}}, \quad (2)$$

here M is the mass and R the radius of the star (in solar units), $\bar{Q}_i$ is a parameter which depends on the physics. For the fundamental mode of models computed with either CHeB or HHeB, an adiabatic seismological analysis gives $\bar{Q}_i \sim 0.0425$, a value consistent with the data of Cox (1980).

Mean values: the Cepheids cross the instability strip with different values of luminosities and periods. Only mean values of these quantities are relevant for comparisons with observations. For each mass value, the calculation of the means proceeds in two steps:

1. for each crossing of the instability strip, the geometric means (arithmetic mean of logarithms) of luminosities and periods are calculated successively for the first section of the evolutionary track where the period (e.g. radius) increases monotonously, then for the second section where the period decreases and so forth;
2. the global means are taken as the weighted means of former ones, taking the durations of each crossings as weights.

3. The evolution of Cepheids with HHeB and CHeB

Figure 2 shows the evolutionary tracks of stellar models of 4−10 $M_\odot$ computed with CHeB (left panel) and HHeB (right panel) respectively. Figure 3 displays the evolutionary tracks (middle panel) and the evolutions of internal structure (top and bottom panels) of 6.6 $M_\odot$ models. Filled areas correspond to convection (mixed) zones, labels are self-explanatory.

For models computed with HHeB, the evolutionary tracks cross the instability strip on the sub-giant branch once (Fig. 2 right panel). The ignition of the 3α reactions coincides with the departure from the Hayashi line (Fig. 2 right panel, Fig. 3 middle panel, flag #A). While helium is burnt in a convective core, the evolutionary track shows excursions, from the Hayashi asymptotic line towards higher effective temperature (flags #A to #B), subsequently coming back towards the asymptotic giant branch as the exhaustion of helium at centre proceeds. Large loops are obtained for stars with large mass. With decreasing mass, the loops become gradually smaller and finally degenerate to a mere down and up along the Hayashi line. For higher masses just before flag #C, the radiative gradient (Eq. (3)) increases above its adiabatic value in the envelope according to a subtle balance between opacity, luminosity, temperature, a fleeting convection zone is formed leading to a blanketing effect. That leads to an enhancement of the core temperature, which is followed by an increase of the effective temperature and by the formation of a supplementary loop (flags #C to #D) finally coming back to the giant branch (flag #E). Sometimes these additional loops (Degl'Innocentini et al. 2008, Fig. 1) are described outside of the instability strip as seen in Fig. 2 right panel for $M \gtrsim 7\ M_\odot$. As the evolutionary tracks cross the instability strip with different luminosity values several times, it is difficult to associate a theoretical model to a defined location in the instability strip. Figure 3 middle panel exhibits such ambiguous situations. Moreover the existence, the formation, the shape, and the extension of blue-loops appear to be caused by the interaction of several factors with an extreme sensitivity to small changes in the stellar chemical composition, in the physics adopted, and in the calculations (Kippenhahn & Weigert 1991, par. 31.4). The same prevails for

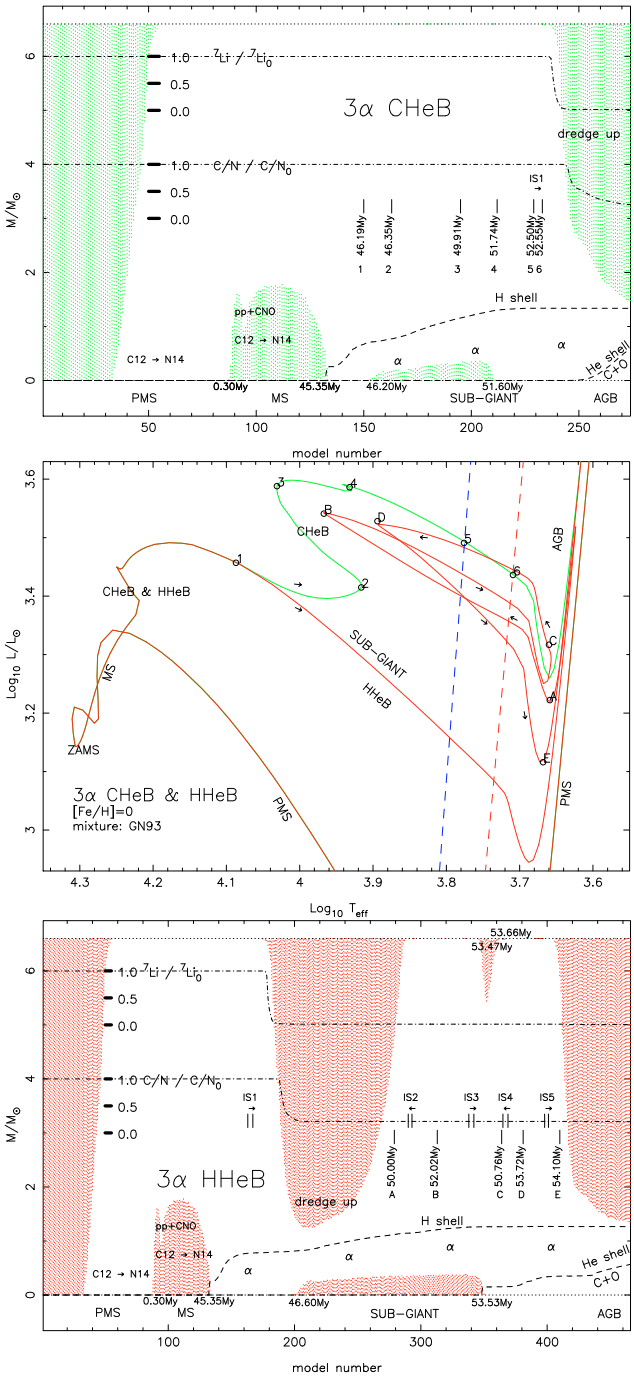

Fig. 3. (Colour online) Evolutions of the internal structure of two models of 6.6 $M_\odot$ calculated with CHeB (*upper panel*) and HHeB (*lower panel*) respectively. *The middle panel* shows their evolutionary tracks. The models are initialized at PMS (ages in Myr). The blue and red borders of the instability strip are indicated by dashed lines. The crossings of the instability strip are mentioned by IS1, IS2, etc. Dash-dot lines are the profiles of atmospheric lithium and C/N ratio normalized to their initial values. Convection zones are indicated by filled areas. Other labels are self-explanatory.

the formation of fleeting convection zones leading to the generation of additional blue loops.

Within the instability strip the luminosity is about constant, so that on the way towards the blue limit the effective temperature increases, while the radius and the period decrease (Eq. (2)), they both increase on the way towards the red part. As reported in Tables 4–6 the temporal derivative of the period, $\dot{p}$, is negative when the star is on the way towards the blue and positive when it goes towards the red.

For models computed with CHeB the situation is simpler. The evolutionary tracks become separated as soon as the 3α is ignited in the core (Fig. 2 middle panel, flag #1). That occurs on the sub-giant branch before any dredge-up. At the centre the temperature is close to $T_c \sim 60$ MK and a convective core is formed. Between flags #1 and #2 the luminosity and the stellar radius increase. At flag #2 the abundance of He is halved in the core. Between flags #2 and #3, the core becomes radiative and Y has decreased to 0.1 at the centre. The star expands and the effective temperature and luminosity increase. The nuclear energy generation amounts to 37% from He burning and 67% from CNO. At flag #4 the temperature at the centre amounts to 100 MK and the stellar radius expands up to $\simeq$17 $R_\odot$; the helium is exhausted at the centre, the core becomes radiative and He starts to burn in a shell source. The evolutionary track undergoes a tiny turn-off. Between flags #5 and #6 the CHeB model crosses the instability strip with a luminosity higher than that of the HHeB model at the beginning of its secondary blue loop (flags #C to #D, then #E). Afterwards, the effective temperature decreases, and the increase of opacity makes the envelope convective. The mixing expands down to the hydrogen shell source and the model goes back to the Hayashi line.

Summing up, the evolutionary tracks cross the instability strip:

- on the sub-giant branch and during helium exhaustion at the centre which occurs *after the dredge-up* for models computed with HHeB.
- after helium exhaustion at the centre, which occurs *before the dredge-up* for models computed with CHeB.

These differences have observable and observed consequences.

4. Discussion

Theoretical mass: the amount of helium processed in the core by nuclear hydrogen burning along the main sequence is identical for CHeB and HHeB. At the ignition of the 3α reactions in models computed with HHeB helium has been already diluted[1] by a deep dredge-up (see Fig. 3 bottom panel). A consequence is a reduced reservoir of nuclear helium fuel, leading to a lesser 3α energy generation and smaller mean luminosity, as seen in Table 1. As already quoted, in the late sixties it became apparent that the theoretical and pulsation masses do not agree. As seen in Fig. 3 (middle panel), the model computed with CHeB crosses the instability strip with the highest luminosity. The mean luminosity values reported in Table 1 confirm this main feature: all models computed with CHeB cross the instability strip with higher mean luminosity than the models of the same mass, but computed with HHeB.

Therefore to a fixed mean luminosity will correspond a smaller mass for models computed with CHeB. Figure 4 shows the linear regressions of mass with respect to period. If the new 3α rate was at work in the stars, the dashed line would correspond to the pulsation mass and the full one to the larger theoretical one. The differences amount to ~0.02 dex (~4.5%). This first approximation goes in the right direction, although the difference does not reach the 10 to 20% required by Keller (2008). Furthermore, the difference is constant with respect to the period which is conform to Keller's inferences – note that Keller removed the mass discrepancy trend with respect to the mass previously found by Caputo et al. (2005).

[1] Because $\log_{10} T_{\rm eff} \lesseqgtr 3.8$, the subsequent increase of atmospheric helium is not observable during the pulsation.

Table 1. Logarithms of the mean luminosity ($L/L_\odot$) for models lying in the instability strip computed with HHeB, CHeB, and CHeBm.

$M/M_\odot$	HHeB	CHeB	CHeBm
4.0	2.440	2.613	2.602
5.0	2.949	3.025	2.964
6.0	3.235	3.300	3.198
7.0	3.470	3.554	3.442
8.0	3.666	3.755	3.747
9.0	3.818	3.939	3.891
10.0	3.926	4.116	4.048

Table 2. Same as Table 1 for the logarithms of mean periods (day).

$M/M_\odot$	HHeB	CHeB	CHeBm
4.0	0.0096 ± 0.025	0.1623 ± 0.063	0.1519 ± 0.025
5.0	0.4317 ± 0.024	0.5222 ± 0.032	0.4447 ± 0.056
6.0	0.6840 ± 0.034	0.7444 ± 0.034	0.6305 ± 0.066
7.0	0.8744 ± 0.072	0.9344 ± 0.040	0.8492 ± 0.050
8.0	1.034 ± 0.089	1.123 ± 0.034	1.109 ± 0.056
9.0	1.124 ± 0.099	1.270 ± 0.046	1.212 ± 0.063
10.0	1.239 ± 0.134	1.400 ± 0.047	1.339 ± 0.069

Duration of the pulsation: Table 3 reports the total durations of the presence in the instability strip of models computed with HHeB and CHeB. Except for the 4 $M_\odot$ exempted of blue-loop and for the 10 $M_\odot$, whose blues loops are mainly off the instability strip, the models computed with HHeB spend more time in the instability strip than the models computed with CHeB. This short duration seems to contredict the existence of so many Cepheids.

Period changes: for all crossings of the instability strip of models computed with HHeB and CHeB, Tables 4 and 5 show the mean values of periods with their signed temporal derivative, $\dot{p}$. These results are consistent with the observed values reported by Turner et al. (2006, Fig. 4) for more than two hundred galactic Cepheids spread out over more than a century of observations. Similar observations of decreases and increases of periods for Cepheids of type II in M 13 and M 5 have been recently reported by Rabidoux et al. (2010). As the models computed with CHeB cross the instability strip with a monotonous increase of the radius, the temporal derivative of the period is always positive. Therefore CHeB is incompatible with the observed large number of Cepheids that have periods with negative temporal derivative.

Lithium and C/N depletion: in models evolved with CHeB, no dredge-up occurs before crossing the instability strip; therefore the atmospheric lithium during the Cepheid phase has kept its initial value. The atmospheric isotopic ratio C/N, which is depleted in the core by the CNO nuclear network at the end of the pre-main sequence, is unchanged. As seen in Fig. 3 upper panel,

Table 3. Total time (Myr) of presence in the instability strip for models computed with HHeB, CHeB, and CHeBm respectively.

$M/M_\odot$	HHeB	CHeB	CHeBm
4.0	0.0703	4.205	5.932
5.0	1.413	0.1640	1.194
6.0	0.5593	0.0435	0.3321
7.0	0.1014	0.0242	0.2612
8.0	0.0458	0.0135	0.2218
9.0	0.0184	0.0154	0.0374
10.0	0.0074	0.0300	0.0276

Table 4. Results of models of different masses computed with HHeB.

$M/M_\odot$	$\log_{10} L/L_\odot$	$\log_{10} p$	$\log_{10} \lvert\dot{p}\rvert$	Δt
4.0	2.440	0.0010	(+)0.6165	0.0703
6.0	2.953	0.4391	(+)0.7586	0.0078
	3.205	0.6688	(−)0.2638	0.1845
	3.248	0.6874	(+)0.0298	0.1115
	3.272	0.7239	(−)0.2278	0.0950
	3.251	0.6874	(+)0.0895	0.1605
8.0	3.395	0.7783	(+)1.622	0.0035
	3.674	1.055	(−)1.186	0.0172
	3.687	1.043	(+)1.408	0.0137
	3.775	1.127	(−)1.621	0.0085
	3.536	0.9000	(+)1.730	0.0031
10.0	3.733	1.051	(+)2.232	0.0017
	4.031	1.344	(−)2.187	0.0046
	3.791	1.099	(+)2.354	0.0011

Notes. Columns 2 and 3 respectively provide the logarithms of the mean luminosity and period calculated by considering independently (1) the first section of the evolutionary track where the period increases monotonously when crossing the instability strip and (2) the section where the period decreases and so forth. Column 4 provides the rate of the period change $\dot{p} = \mathrm{d}p/\mathrm{d}t$ (in seconds per year) and its sign is denoted by "+" or "–". Column 5 gives the duration of the crossings Δt (in Myr).

the atmospheric abundance of ^{7}Li and the C/N ratio have kept their initial values when the model of a 6.6 $M_\odot$ star crosses the instability strip. On the contrary, for the model computed with HHeB, due to the deep dredge-up occurring along the evolution on the Hayashi line, they are already depleted when the model crosses the instability strip. In Cepheids atmospheres, the observed depletion of C/N has long been attributed to a dredge-up occurring before the helium burning in the core (Luck & Lambert 1981). Several authors have reported an unexplained existence of atmospheric lithium in many giants around the instability strip (Luck & Lambert 1981; Kovtyukh et al. 2005) and in the blue side of the HR diagram (Charbonnel & Balachandran 2000). Two Cepheids are lithium-rich, most others are not. A presently no process confident explains the presence of lithium in these stars. Though the new 3α rate could contribute to an explanation of presence of atmospheric lithium, as the C/N ratio is always observed to be depleted, there is a need for a deep dredge-up prior to the pulsation phase for Cepheids.

5. Numerical experiences

The study of Dotter & Paxton (2009) and the present analysis show that models computed with CHeB do not agree with observations. However, the new 3α reaction rate, based on the direct solution of the Schrödinger equation, has a paramount theoretical interest, which deserves care.

Table 5. Same as Table 4 for the models computed with CHeB.

$M/M_\odot$	$\log_{10} L/L_\odot$	$\log_{10} p$	$\log_{10} \lvert\dot{p}\rvert$	Δt
4.0	2.460	0.0277	(+)0.6655	0.0708
	2.542	0.1059	(−)1.941	2.162
	2.696	0.2289	(+)1.687	1.972
6.0	3.300	0.7444	(+)0.5086	0.0435
8.0	3.775	1.123	(+)1.383	0.0135
10.0	4.116	1.400	(+)1.443	0.0030

Table 6. Same as Table 4 for the models computed with CHeBm.

$M/M_\odot$	$\log_{10} L/L_\odot$	$\log_{10} p$	$\log_{10} \lvert\dot{p}\rvert$	Δt
4.0	2.433	0.0202	(+)0.5898	0.0425
	2.591	0.1418	(−)2.288	4.798
	2.659	0.2011	(+)1.584	1.092
6.0	3.106	0.5644	(+)0.2485	0.0608
	3.170	0.6009	(−)0.1957	0.1814
	3.317	0.7348	(+)0.0884	0.0899
8.0	3.589	0.9536	(+)1.157	0.0190
	3.676	1.036	(−)1.181	0.0219
	3.765	1.132	(+)0.8726	0.0574
	3.780	1.139	(−)0.7767	0.0838
	3.765	1.127	(+)0.9062	0.0399
10.0	3.889	1.173	(+)2.072	0.0040
	4.092	1.381	(−)2.150	0.0068
	4.069	1.362	(+)1.720	0.0168

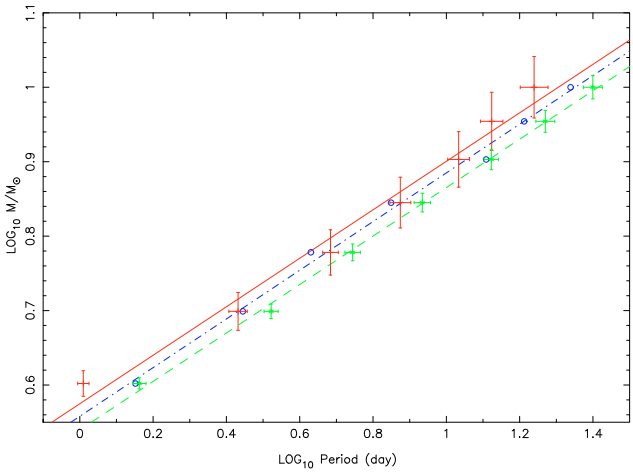

Fig. 4. (Colour online) Mass-period relationship for theoretical models computed with CHeB (dashed), HHeB (full), and CHeBm (dot-dash) respectively.

As far as the Cepheids are concerned, the touchstone is the existence of a deep dredge-up before the ignition of the 3α reactions. With CHeB these conditions might be filled if the occurrence of the helium ignition was translated towards the Hayashi line. This could be obtained if the correction of Ogata et al. (2009) was slightly reduced, because the CHeB rate goes to the HHeB one as $\Delta 3\alpha$ goes to unity. On the other hand, because the activation of the convection is monitored by the radiative temperature gradient:

$$\nabla_{\mathrm{rad}} = \frac{3}{16\pi acG}\frac{\kappa LP}{MT^4}, \qquad (3)$$

either an increase of the metallicity, which enlarges the opacity κ, or a core-overshooting, which increases the reservoir of nuclear energy and then the luminosity L, might induce more efficient

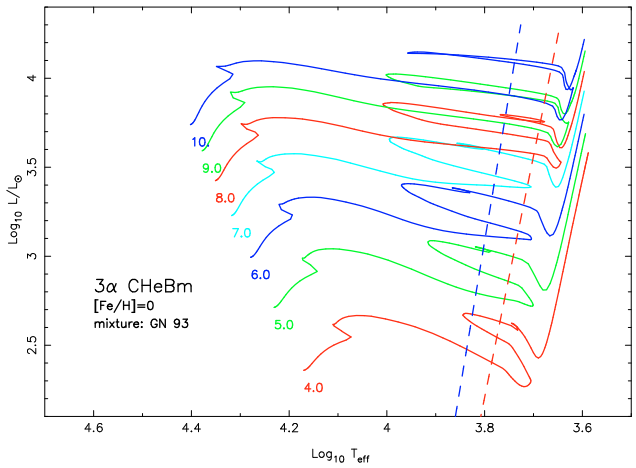

Fig. 5. (Colour online) Same as Fig. 2 *left panel* for CHeBm (modified 3α OKK rate).

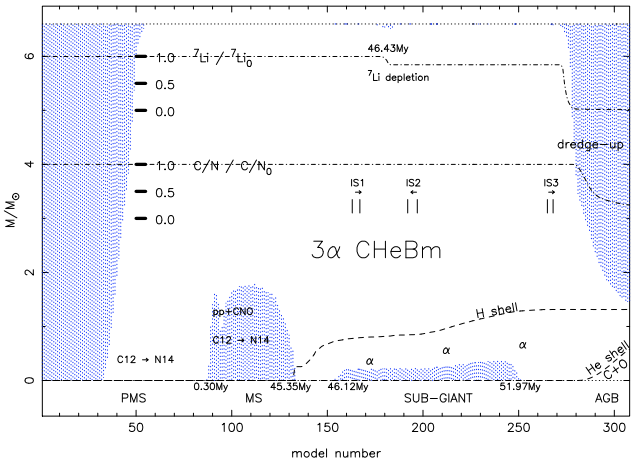

Fig. 6. (Colour online) Evolution of the internal structure of a 6.6 $M_\odot$ model computed with CHeBm.

convective instability (in Eq. (3), P is the pressure, T the temperature, a the radiative constant, G the gravity constant and c the speed of light).

• Reduction of $\Delta 3\alpha$. We arbitrarily change the OKK correction in the following way:

$$\log_{10}(3\alpha_{\rm CHeBm}) = \log_{10}(3\alpha_{\rm NACRE}) + 0.97 \times \log_{10}(\Delta 3\alpha), \qquad (4)$$

This modified rate, referenced by CHeBm (*modified cold helium burning*) is shown in Fig. 1, while Fig. 5 shows the evolutionary tracks. Tables 1–3 allow comparisons between the relevant characteristics of the models. For models computed with HHeB and CHeBm, the durations into the instability strip are of the same order, the mean luminosities are only slightly higher for CHeB models, and even lower for some masses. The CHeBm models present several crossings of the instability strip with sign changes of the temporal derivative of the period. Between the first and the second crossing (flags IS1 to IS2 in Fig. 6) a slight enlargement of the outer convection zone occurs. It comes down to a level at which lithium is depleted but not deep enough to scoop up the material processed in the core by the CNO cycle, therefore the atmospheric ratio C/N remains unchanged.

• Increase/decrease of the metallicity. The evolutionary tracks of the 6.6 $M_\odot$ models CHeB+, CHeB– shown in Fig. 7 are computed with high metallicity ($X = 0.7019$, $Y = 0.2700$, $Z = 0.02808$, $Z/X = 0.04$) and low metallicity ($X = 0.7264$, $Y = 0.2700$, $Z = 0.003632$, $Z/X = 0.005$) respectively. The model CHeB+ crosses the instability strip several times but has no significant dredge-up, therefore atmospheric lithium and C/N ratio are not depleted. Furthermore a metallicity this high is not observed. The evolutionary track of the model CHeB – is translated towards the blue side of the HR diagram and does not reach the instability strip prior to the helium exhaustion at the centre.

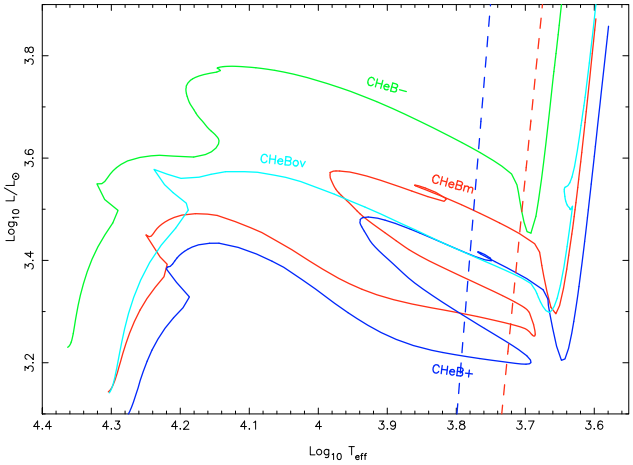

Fig. 7. (Colour online) Comparisons of evolutionary tracks of 6.6 $M_\odot$ models of numerical experiences, see Sect. 5.

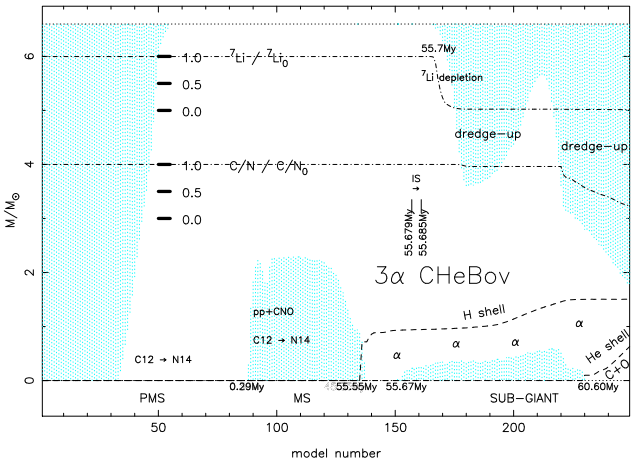

Fig. 8. (Colour online) Evolution of the internal structure of a 6.6 $M_\odot$ model computed with CHeBov (overshooting).

• Convective core overshooting. The 6.6 $M_\odot$ model labelled CHeBov is computed with CHeB and a convective core extension amounting to $Ov = \Lambda_{\rm ov} \min(H_{\rm P}, R_{\rm co})$, ($H_{\rm P}$ is the pressure scale height, $R_{\rm co}$ the radius of the convective core) and $\Lambda_{\rm ov} = 0.25$. In the mixed extension the temperature gradient is taken to be the radiative one. As seen in Fig. 8 the first dedge-up occurs after the crossing of the instability strip. The extension of the mixing is not deep enough to reach the core and atmospheric C/N ratio is not depleted. On the other hand, no blue loop is formed.

6. Conclusions

In this paper we have examined some consequences of the new rate of the 3α nuclear reaction rate derived by Ogata et al. (2009) for models of intermediate mass stars. Because the temperature of the ignition of the 3α reactions is about halved, the helium burning starts on the sub-giant branch, about midway towards the Hayashi line. Owing to the high efficiency of the new rate, helium burns in the core before the occurrence of any dredge-up with the consequences:

- it is no longer necessary to have blue-loops with a large enough extent for crossing the instability strip;
- the evolutionary tracks cross the instability strip once and only once with a practically constant luminosity. There is a once to once mapping between luminosity, effective temperature and mass, age;
- because helium is not diluted by a deep dredge-up, the large amount of helium nuclear fuel available in the core leads for a given mass to a higher luminosity. Hence the difference between theoretical and pulsational mass is reduced. *Potentially*, for some Cepheids, the estimated distance from the theoretical luminosity/period relationship might be reduced.

On the other hand, several properties of models contradict the observations of a century and concerning more than two hundred Cepheids:

- the more serious is the *positive* rate of the period change caused by the monotonous enlargement of the radius during the crossing of the instability strip. The observations clearly exhibit *positive and negative* rates of period change.
- observations also reveal the depletion of the atmospheric lithium and C/N ratio, consequences of a deep dredge-up occurring *before* the pulsation phase, but occuring later in models computed with the new 3α rate.

These two unquestionable observational facts argue against the pertinence of the 3α rate of Ogata et al. (2009). In another connection, we find that only a slight change of this rate towards the NACRE value could be sufficient to restore changes of the sign of temporal derivatives of periods. Owing to its theoretical interest, the 3α new rate of Ogata et al. (2009) deserves to be revisited and Cepheids will offer quantitative tests. In this respect many observational inputs are expected from space missions CoRoT and Kepler for seismology and Gaia for distances.

Acknowledgements. We express our gratitude to the referee Dr. Nielson whose important and constructive remarks led to substantial improvements of the paper.

References

Alexander, D. R., & Ferguson, J. W. 1994, ApJ, 437, 879
Angulo, C., Arnould, M., Rayet, M., & the NACRE collaboration 1999, Nucl. Phys. A, 656, 3
Asplund, M., Grevesse, M., & Sauval, A. J. 2005, in Cosmic Abundances as Records of Stellar Evolution and Nucleosynthesis, ed. T. G. Barnes III, & F. N. Bash, ASP Conf. Ser., 336
Canuto, V. M., & Mazitelli, I. 1991, ApJ, 370, 295
Caputo, F., Bono, G., Fiorentino, G., Marconi, M., & Musella, I. 2005, ApJ, 629, 1021
Charbonnel, C., & Balachandran, S. C. 2000, A&A, 359, 563
Cox, A. N. 1980, ARA&A, 18, 15
Degl'Innocentini, S., Prada Moroni, P. G., Marconi, M., & Ruoppo, A. 2008, Ap&SS, 316, 25
Dotter, A., & Paxton, B. 2009, A&A, 507, 1617
Eggleton, P. P., Faulkner, J., & Flannery, B. P. 1973, A&A, 23, 325
Grevesse, N., & Noels, A. 1993, in Cosmic Abundances of the Elements, ed. E. Prantzos, Langioni-Flam, & M. Casse (Cambridge Univ. Press), 14
Iben, I. 1975, ApJ, 196, 525
Iglesias, C. A., & Rogers, F. J. 1996, ApJ, 464, 943
Keller, S. C. 2008, ApJ, 677, 483
Kippenhahn, R., & Weigert, A. 1991, Stellar Structure and Evolution (Berlin: Springer-Verlag)
Kovtyukh, V. V., Wallerstein, G., & Andrievky, S. M. 2005, PASP, 117, 1182
Luck, E. R., & Lambert, D. L. 1981, ApJ, 245, 1018
Mihalas, D. 1978, Stellar Atmosphere (New York: Freeman and Cie)
Morel, P. 1997, A&AS, 124, 597
Morel, P., & Lebreton, Y. 2008, Ap&SS, 316, 61
Ogata, K., Kan, M., & Kamimura, M. 2009, Prog. Theor. Phys., 122, 1055
Saruwatari, M., & Hashimoto, M. 2008, Prog. Theor. Phys., 120, 1
Rabidoux, K., Smith, H. A., Pritzl, B. J., et al. 2010, ApJ, 139, 2300
Turner, D. G. 2001, Odessa Astr. Pub., 14, 166
Turner, D. G., Abdel-Latif, M. A.-S., & Berdnikov, L. N. 2006, PASP, 118, 410
Valle, G., Marconi, M., Deg'Innocenti, S., & Prada Morono, P. G. 2009, A&A, 507, 1541